Tellus (2000), 52B, 620–635
Printed in UK. All rights reserved

TELLUS
ISSN 0280–6509

Polarising properties of the aerosols in the north-eastern tropical Atlantic Ocean, with emphasis on the ACE-2 period

By THIERRY ELIAS*, CLAUDE DEVAUX, PHILIPPE GOLOUB and MAURICE HERMAN,
Laboratoire d'Optique Atmosphérique, 59655 Villeneuve d'Ascq, France

(Manuscript received 11 February 1999; in final form 11 October 1999)

ABSTRACT

Measurements of the polarisation state of the atmosphere were performed at Tenerife in June–July 1997, in the framework of ACE-2 (second Aerosol Characterization Experiment), by 2 ground-based instruments: RefPol (a LOA prototype) which took measurements at 445, 665, 870, 1610 nm in the solar principal plane; and an automatic CIMEL (CE 318) sun/sky-photometer which measured polarised radiation at 870 nm in the same observational geometry. Measurements acquired during the campaign, as well as AERONET (AErosol RObotic NETwork) measurements acquired at the sites of Cape Verde and M'Bour, are processed with an algorithm determining the polarised single-scattering sky-radiance due to aerosols, directly proportional to the aerosol polarised phase function (representing the probability to scatter polarised radiation in the direction of the scattering angle). A good correlation between the Ångström exponent α, representing the spectral dependence of the extinction measurements, and the polarised phase function is observed on each set of data. The uncertainty of retrievals at 445 nm makes the determination of the spectral dependence of polarisation inconclusive but does not prevent confirming the dependence of the aerosol polarised phase function on α, at all wavelengths. An Ångström exponent of 1 corresponds to a polarised phase function of around 0.1 (± 0.04), at 870 nm and at a scattering angle of 60°. For α between 0 and 0.4, the average value of the polarised phase function is 0.05. The correlation shows that polarisation is more sensitive to small particles than to large particles. The discrepancy between retrievals and Mie calculations from an AERONET size distribution, inverted from Izaña measurements acquired during a dust event, suggests the presence of small particles, not detected by total sky-radiance measurements.

1. Introduction

The strong interaction between solar radiation and the atmospheric aerosols addresses the reason why, and the way how we study their radiative effect. Indeed the size range of the aerosol particles make them significantly influence the global radiative budget of the atmosphere–Earth system and allows us to observe the aerosols by means of photometry.

Aerosols are mainly located in the lower troposphere, but their spatial distributions are very dependent on sources and sinks, and on their lifetime (a few days to a week in the troposphere), which is very short compared to the greenhouse gases. Therefore the climatological impact of aerosols is strongly regional. However, large scale transport (Saharan aerosol dust, volcanic eruption), and areas of intensive continuous production of particles (anthropogenic pollution from the

* Corresponding author.
e-mail: elias@loa.univ-lille1.fr

industrialised regions of the world) extend the influence of the aerosols in global zones. Therefore, heliosynchronous satellites are very suitable tools for investigating aerosol characteristics. However, ground based, shipborne and airborne measurements of the atmospheric radiation as provided by instruments attached in networks, or during intensive field campaigns, are necessary in order to complete and validate the satellite surveys.

In this context, ACE-2 (the second Aerosol Characterisation Experiment) took place in Tenerife (28°18′N 16°29′W) in June–July 1997. The experiment was designed to investigate the physical and chemical characteristics of aerosols (Verver et al., 2000; Raes et al., 2000). In particular, dust aerosols were investigated, as their importance in the global radiative budget is expected (Tegen and Lacis, 1996). Tenerife was chosen as the major platform for ACE-2 operations, as it is located in the north-east tropical Atlantic Ocean, in the outflow region (10°–30°N) of Saharan desert dust to Central America (Prospero and Carlson, 1972).

Radiative measurements of planetary atmospheres (Hansen and Hovenier, 1974) and simulations (Cairns et al., 1997; Mishchenko and Travis, 1997) show that polarisation, induced by scattering processes, can provide precise information on aerosol microphysics. Polarisation measurements are well adapted to aerosol retrieval over land as surface influence in polarisation is small, specially compared to its effect on sky-radiance (Bréon et al., 1995; Deuzé et al., 1993; Herman et al., 1997).

Measurements of the atmospheric extinction of the solar light were performed at visible and near infrared wavelengths in two sites in Tenerife by two instruments from L.O.A. (Laboratoire d'Optique Atmosphérique): at sea level in Santa Cruz De Tenerife; and at 600 m a.s.l. (above sea level) in San Cristobal De La Laguna. Moreover multispectral measurements of the polarisation state of the atmosphere were acquired by an L.O.A. prototype and by a CIMEL (model CE-318) sun/sky photometer, owned by L.O.A., and equipped with polarisers at 870 nm. Polarisation data were acquired in the two prequoted sites, as well as in Izaña, the main platform of ACE-2 measurements in Tenerife (Smirnov et al., 1998; Russell and Heintzenberg, 2000; Welton et al., 2000).

RefPol (for Reflectance and Polarisation), the L.O.A. prototype, has been developed for the validation of the POLDER (POLarization and Directionality of Earth Reflectance (Deschamps et al., 1994)) instrument, which was first set up onboard aircraft, and then launched in September 1996 onboard the Japanese spatial platform ADEOS (Advanced Earth Observing Satellite). During the POLDER survey, RefPol measurements were performed in Lille (50°36′N 3°8′E, 60 m a.s.l.), an urban area, from January 1997, and in Tenerife during ACE-2. Also, since 1994, polarised photometers (CIMEL type) have run world wide as part of the ground-based AERONET (AErosol RObotic NETwork) network (Holben et al., 1998), and in particular in M'Bour (Senegal) and Cape Verde, which are two sites located in the same area as Tenerife, and also impacted by the Saharan dust aerosols.

An algorithm, developed at near infrared wavelengths by Vermeulen (1996), is used to retrieve the polarised phase function from the combination of the measured polarised sky radiance and the aerosol optical thickness, and extended to visible wavelengths. The polarised phase function is the angular probability of a particle to scatter polarised light in the direction of the scattering angle, therefore only represents the polarising properties of the aerosols (without influences of the experimental characteristics, particle quantity, molecular contribution, ...). It corresponds to the P_{12} element of the aerosol phase matrix $\boldsymbol{P}$, which is a Mueller matrix composed of 16 elements (4×4) (Lenoble, 1993). It is dimensionless, as the natural phase function (Van de Hulst, 1957), which corresponds to the P_{11} element of the phase matrix and which is normalised as

$$\frac{\int_{\text{space}} P_{11}(\Theta, \Phi)\, \mathrm{d}\omega}{4\pi} = 1;$$

Θ, Φ are the zenith and azimuth angles respectively; $\mathrm{d}\omega$ is an infinitely small solid angle, in steradians, and 4π represents the complete solid angle (steradians). In the adopted formalism, polarisation is positive when the polarisation direction is perpendicular to the incident plane (which contains the solar and scattering directions), negative when it is parallel.

The dependence of results on the Ångström exponent, independently measured and indicative

of the size distribution, is revealed by measurements in Tenerife, and in M'Bour and Cape Verde. The spectral dependence of the polarised phase function inferred from measurements in Tenerife is discussed. Finally, our polarisation data are compared with the polarisation inferred from Mie calculations with an AERONET-inverted size distribution.

2. Experimental

2.1. Site description

To investigate the influence of desert aerosol on the polarisation state of the atmosphere, three measurement sites in the north-eastern tropical Atlantic Ocean are selected: Tenerife (28°18′N 16°29′W), M'Bour (14°23′N 16°57′W) and Sal Island (16°45′N 22°57′W). These sites are located far from sources of urban and industrial pollution, and in the westerly outflow of Saharan desert aerosols. Their geographical characteristics relevant to this study are briefly discussed.

For more than a decade, Tenerife has supported measurements for dust surveys (Arimoto et al., 1995). Tenerife is a volcanic island of the Canary archipelago, 400 km offshore the Moroccan coasts. The interaction of Azores high and the Canaries cold stream produces a subsidence inversion layer usually situated between 1200 and 2000 m a.s.l., which hinders the arrival of Marine Boundary Layer (MBL) pollution in the Free Troposphere (FT) (Raes et al., 2000). During the ACE-2 campaign, three sites were chosen on the island for acquiring polarisation data. The first is located in the FT, at the Izaña Observatory (2367 m a.s.l., hereafter Izaña), and two others in the MBL, at two different altitudes, in Santa Cruz De Tenerife(0 m a.s.l., hereafter Santa Cruz) and San Cristobal De La Laguna (600 m a.s.l., hereafter La Laguna). Izaña is a Global Atmospheric Watch (GAW) station, as well as a major ACE-2 platform (Smirnov et al., 1998; Raes et al., 2000; Welton et al., 2000).

Santa Cruz is the capital of the island, situated on the north-eastern coast. Measurements were taken at the Nautical School of Santa Cruz, directly on the coast. The site is under the influence of north-westerly clean maritime air, which prevents the influence of urban pollution on the site.

La Laguna is the second major town of the island on the slope hillside of the mountain chain of Anaga, at 600 m a.s.l.. Two major local sources of pollution impact the site located on the roof of the Universidad de Fisica e Matematica: intense road traffic and the International North airport. Santa Cruz and La Laguna are located 10 km apart. Meteorological centres are located in vicinity of each site.

2 sites part of the AERONET network are located in the area. One is at Sal Island, the most north-eastern island of Cape Verde archipelago, 500 km offshore the Senegalese coast. Measurements of atmospheric extinction have been performed since 1991 (Chiapello et al., 1997; Chiapello et al., 1999). The sampling site is located at 60 m a.s.l., 7 km away from a town of 25000 inhabitants. The other site is located at the same longitude, but closer to the source of the desert aerosols, subject to maritime influence as well, at M'Bour, 80 km south of Dakar (capital city of Senegal). This site is at sea level, directly on the shore, and surrounded by a Sahel-type vegetation.

2.2. Instrumental

3 instruments belonging to L.O.A. were run in Tenerife from 15 June until 22 July 1997: a L.O.A.-prototype polarimeter, denominated RefPol (Reflectance and Polarisation), a manual CIMEL sunphotometer and an automatic CIMEL (CE-318) sun/sky photometer, labelled respectively LOA-manual and LOA-71. An AERONET CIMEL, labelled here NASA-02, acquired data in Izaña. The AERONET sites of Cape Verde and M'Bour are equipped with two automatic CIMEL sun/sky photometers, running from February 1996 to February 1998, and from December 1996 to August 1997, respectively.

RefPol takes multispectral measurements of the total and polarised sky-radiances (quotient of polarised over total radiance provides the degree of polarisation) of the atmosphere at 445, 665, 870 and 1610 nm in the principal plane.

All CIMEL instruments measure aerosol optical thickness at 445, 665, 870, 1020 nm. Except LOA-manual, all CIMEL's operate automatically, and measure as well sky-radiance in the almucantar and solar principal plane geometry at 445, 665, 870, 1020 nm, while the polarised radiance is measured only at 870 nm in the solar principal plane (Holben et al., 1998).

RefPol and the automatic CIMEL's (as POLDER) measure polarisation according to the same principle: the linearly polarised component of the light is measured with polarising filters mounted on a rotating wheel. For calculating the polarisation rate, three measurements of the polarised light are acquired in correspondence of three positions of the rotating wheel. In case of CIMEL (and POLDER), these three measurements are spaced of 60°, in the case of RefPol, of 45°. These measurements are then combined to give the total and the polarised radiances. The total radiance L_{tot} corresponds to the first component of the four Stokes parameters (Lenoble, 1993), while the polarised radiance is related to the three others. Concerning the atmospheric conditions, the fourth parameter is negligible compared to the others, which means that atmospheric polarisation is mostly linear. Therefore the polarised radiance depends on the second and the third Stokes parameter as $L_{pol} = \sqrt{Q^2 + U^2}$ (Lenoble, 1993).

Measurements are made for cloudless atmospheric conditions, from the ground. The sweeping motion is included in the solar principal plane, which is the plane perpendicular to the Earth's surface and containing the sun. The instrumental viewing angle θ_V ranges between $-90°$ and $+90°$, with respect to the zenith position. The scattering angle is defined as $\theta_d = \theta_V + |\theta_S|$, where θ_S is the solar zenith angle. Therefore, in the principal plane, θ_d ranges between 0 and $|\theta_S| + 90°$.

2.3. Measurement validation in Tenerife

Days for which measurements are available in Tenerife are reported in Table 1. Visual observations, confirmed by measurements (Smirnov et al., 1998; Formenti et al., 2000; Welton et al., 2000), situate three major dust episodes on 7–9 July, on 17 July and on 23 July during the ACE-2 campaign. In the following, we will mention the other days as "clear days", as opposed to the dust events. Table 2 summarises the experimental characteristics of the measurements discussed throughout the paper (instantaneous values of the aerosol optical thickness, the Ångström exponent, the solar zenith angle, time and location).

Calibration of LOA-71 was performed before and after the campaign at L.O.A. by the Photon team, the European branch of AERONET. RefPol performances are checked regularly at L.O.A. for more than two years.

Two kinds of calibration coefficients are defined for inferring the sky-measurements. Total radiance measurements are affected by the energy calibration coefficients while the degree of polarisation depend on the polarisation calibration coefficients. Therefore polarised radiance results of both kinds

Table 1. *Available polarisation measurements in Tenerife (simultaneous to extinction measurements)*

	Santa Cruz	La Laguna	Izaña
20 June			LOA-71/RefPol, *NASA-02*
21 June			LOA-71/RefPol, *NASA-02*
27 June	LOA-71		
30 June	LOA-71	RefPol, *LOA-manual*	
1 July	LOA-71	RefPol, *LOA-manual*	
6 July	LOA-71	RefPol, *LOA-manual*	
8 July		RefPol, *LOA-manual/LOA-71*	
9 July		LOA-71	RefPol, *NASA-02*
13 July		RefPol, *LOA-71*	
17 July	LOA-71		RefPol, *NASA-02*
18 July	LOA-71		
20 July	LOA-71		
21 July	LOA-71		
22 July	LOA-71		

The instrument of which label is written in italic was used for providing the extinction measurements. The dates in bold frame correspond to dust events occurred in Tenerife during ACE-2. When just the optical thickness data were used, the label of the performing instrument is written in italics.

Table 2. *Summary of the experimental characteristics of data discussed in the paper and encountered in Tenerife during ACE-2; instantaneous values (date and GMT time) of the aerosol optical thickness, the Ångström exponent, the solar angle*

Time	Site	Aerosol optical thickness δ_{aer} at 870 nm	Ängström exponent α	Solar zenith angle θ_S
15 June, 09:27	Izaña	not available	not available	48.5°
20 June, 18:43	Izaña	0.01	1.50	74.4°
30 June, 17:08	La Laguna	0.03	0.93	54.0°
30 June, 17:23	La Laguna	0.03	1.11	57.1
30 June, 18:29	La Laguna	0.04	1.50	71.3°
01 July, 07:56	La Laguna	0.015	1.49	69.0°
08 July, 07:18	La Laguna	0.27	0.25	77.5°
08 July, 08:27	La Laguna	0.25	0.23	63.0°
09 July, 12:12	La Laguna	0.19	0.01	14.3°
17 July, 15:24	Santa Cruz	0.35	0.19	30.4°
17 July, 18:26	Izaña	0.20	0.13	70.7°
20 July, 11:21	Santa Cruz	0.05	−0.03	26.1°

of calibration coefficients. Consequently, the accuracy of RefPol polarised radiance is 7% at 445 and 665 nm, 9% at 870 and 1610 nm. Between each successive evaluation at every wavelength, the calibration coefficients in total radiance stay, however stable, within 5%.

The energy calibration coefficients are computed so as to obtain sky-radiance measurements normalised to the extra-terrestrial solar radiance. Thus the measurements are dimensionless and are independent on the seasonal variation of the distance Earth–Sun. The provided quantity is equivalent to

$$L(\theta_d, \lambda) = \frac{\pi L^*(\theta_d, \lambda)}{E_S(\lambda)},$$

where $L^*(\theta_d, \lambda)$ has radiance units (W m^{-2} sr^{-1} μm^{-1}) and $E_S(\lambda)$ is the monochromatic extra-terrestrial solar irradiance (W m^{-2} μm^{-1}) which depends on the acquisition date. As π is in steradians, $L(\theta_d, \lambda)$ is dimensionless. Throughout the paper all discussed (total and polarised) radiance quantities will be normalised radiance, but for clarity purpose, the term "normalised" will be skipped.

Inter-comparison of RefPol and LOA-71 were performed during 15 June 1997 (a clear day) and during 8 July 1997 (dust event). Total sky radiance is compared at 445, 665 and 870 nm. The measured radiances are plotted in Figs. 1, 2 as a function of the scattering angle. The corresponding values of angularly averaged ratio R^{tot} of total sky-radiance acquired by RefPol over total sky-radiance

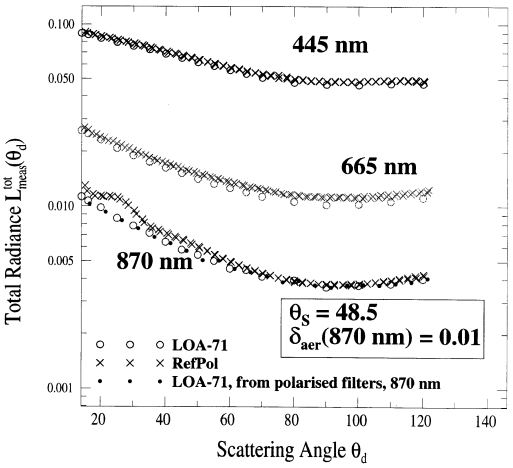

Fig. 1. Total sky-radiance as a function of the scattering angle, measured by RefPol and LOA-71 at the same wavelengths (445, 665, 870 nm) during clear conditions, at Izaña, on 15 June. The dots represent the total sky-radiance inferred from the measurements from the 870 nm-polarising filters of LOA-71.

acquired by LOA-71 are gathered in Table 3. The agreement is good, less than 5% of difference at 445 nm, between 4% and 8% at 665 nm, and around 6% at 870 nm.

The degree of polarisation corresponding to clear and dusty atmospheric conditions, as acquired by RefPol and LOA-71 at 870 nm, are plotted in Fig. 3. While LOA-71 measurements are more scattered, the instruments are coherent

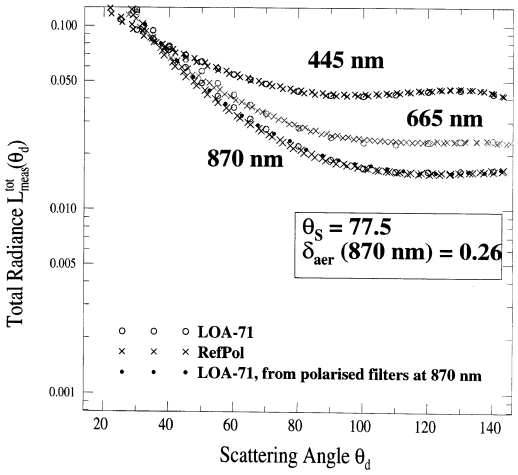

Fig. 2. Same as Fig. 1 except that the measurements were taken during a dust event, in La Laguna, 8 July morning. Both *x*- and *y*-axis have the same scales as in Fig. 1.

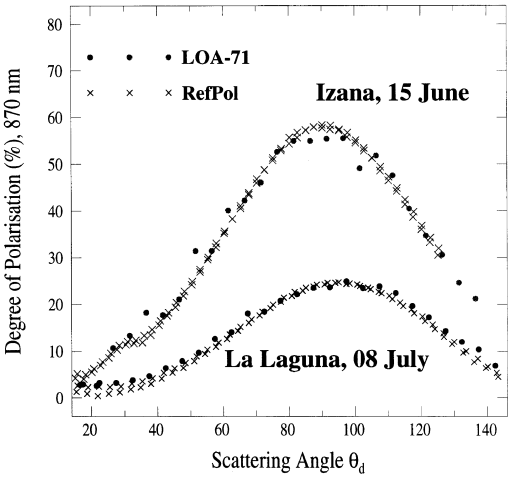

Fig. 3. Degree of polarisation as a function of the scattering angle, measured at 870 nm by RefPol and LOA-71 during a clear day at Izaña and a dust event at La Laguna. Corresponds to the measurements plotted in Figs. 1, 2.

Table 3. *Angularly-averaged ratio, R^{tot}, of total radiance measured by RefPol over total radiance measured by LOA-71, at 445, 665, 870 nm, during an aerosol event and during a clear day; corresponds to measurements plotted in Figs. 1, 2*

R^{tot}	445 nm	665 nm	870 nm
Izaña, 15 June	1.04	1.08	1.07
La Laguna, 08 July	0.99	0.96	0.94

together. The angularly averaged difference is lower than 10%. We can notice the evident strong dependence of the degree of polarisation on the atmospheric conditions (degree of polarisation lower during the dust event).

Because instrumental inter-comparison in polarisation is possible only at 870 nm, we used simulations for validating the polarisation measured by RefPol at 445 nm. This wavelength is chosen as the molecular contribution is dominating, and the signal depends very little on the aerosol model chosen when the aerosol load is small. These conditions are reached on 20 June at Izaña (aerosol optical depth $\delta_{aer}(445\text{ nm}) = 0.02$). To show the weak impact of aerosol polarisation in these conditions, we use the additivity property of aerosol and molecular contributions in polarised radiance (Vermeulen, 1996). A specific phase matrix describes the angular optical properties of each atmospheric constituent: aerosols and molecules. The contribution of molecules in atmospheric polarised radiance is calculated by cancelling the P_{12} term of the aerosol phase matrix $\boldsymbol{P}_a$. Thus, molecules and aerosols scatter the radiation, but only molecules polarise. The aerosol contribution is computed following the same procedure: the P_{12} element of the molecular phase matrix $\boldsymbol{P}_m$ is put equal to 0. It has been noticed that the sum of each contribution equals the atmospheric polarised radiance (calculated without cancelling the aerosol or the molecular P_{12} term), and at every wavelength from 445 to 1610 nm (whereas molecules and aerosols are coupled in total radiance). Respective contributions related to the case study of 20 June is reported in Fig. 4, which shows that aerosols contribute only up to 4% to the atmospheric signal. The comparison between the polarised sky-radiance calculated for the atmosphere and the polarised sky-radiance measured at 445 nm shows that simulation underestimates the measurement up to a scattering angle of 120°. The absolute discrepancy is less than 5%.

If not specified by "aerosol" or "molecule", polarised sky-radiance will concern the scattering processes induced by all the elements composing the atmosphere (aerosols and the molecules).

In the following, only measurements at 445 and

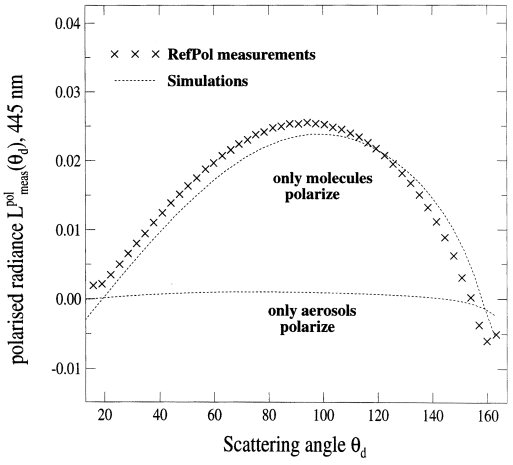

Fig. 4. Polarised sky-radiance as a function of the viewing angle, measured at 445 nm during a clear day at Izaña (20 June) and simulated polarised radiance in the experimental conditions for inter-comparison. Separate contributions of aerosol and molecules in polarised radiance are reported.

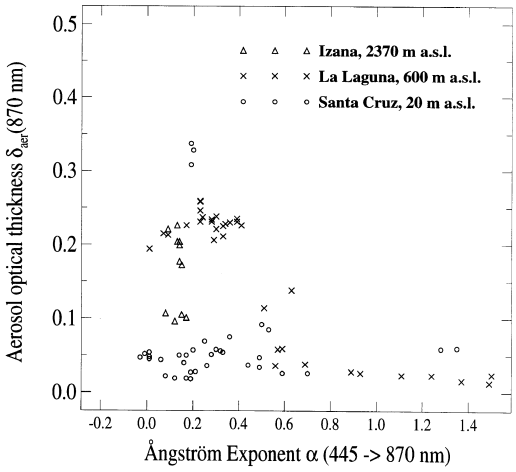

Fig. 5. Representation of the extinction characteristics in Tenerife as the aerosol optical thickness δ_{aer} at 870 nm versus the Ångström exponent α (between 445 and 870 nm).

870 nm will be discussed, as these are the wavelengths, over the four available, at which measurements could be best validated. Moreover extinction measurements are not available at 1610 nm, what makes the interpretation of RefPol measurements at this wavelength difficult. The spectral range of these measurements is sufficient for reporting on the spectral properties of the aerosol polarisation.

3. Extinction measurements

In Fig. 5, the aerosol optical thickness δ_{aer}, measured at 870 nm at Tenerife, is plotted versus the Ångström exponent α, which represents the spectral dependence of δ_{aer} (between 445 and 870 nm in this paper) and which is indicative of the size distribution of the particles. Only extinction measurements acquired simultaneously to the polarisation measurements are shown in Fig. 5.

Data from Izaña were acquired by the AERONET instrument, NASA-02, on 9 and 17 July when RefPol was run at the same place. Data from La Laguna and Santa Cruz were collected by LOA-71 and LOA-manual. The shape of the point cluster is representative of sites impacted by desert aerosols. The large range of Ångström exponent values (from 0.4 to 1.5) corresponds to small values of the aerosol optical thickness (0.01–0.1). These data were acquired during clear days in Santa Cruz and La Laguna. Small values of α (from -0.03 to 0.4) with bigger δ_{aer} (0.1–0.34) correspond to the dust episodes. This is confirmed by the results of other photometric measurements acquired in Tenerife during ACE-2 (Smirnov et al., 1998; Schmid et al., 2000; Formenti et al., 2000). The other data (small value of α and δ_{aer}) were acquired in Santa Cruz. The smallest values of α (Table 2) are obtained from measurements in Santa Cruz on 20 July ($-0.03 < \alpha < 0.06$ for $0.044 < \delta_{aer} < 0.054$) and in La Laguna on 9 July during the 1st dust event ($\alpha = 0.01$ for $\delta_{aer} = 0.19$). The biggest values of α are seen in La Laguna on 30 June afternoon and 1 July morning ($\alpha = 1.50$ for $\delta_{aer} = 0.04$ and $\delta_{aer} = 0.015$, respectively). The aerosol optical thickness measured in Tenerife simultaneously to the polarisation measurements reaches its maximal value in Santa Cruz during the 2nd aerosol event, on 17 July ($\delta_{aer} = 0.34$ for $\alpha = 0.19$).

Similar characteristics are observed even when seasonal variations are incorporated, as for extinction data acquired at Cape Verde and M'Bour (Fig. 6), where the measurement period extends to almost 3 years. The scatterplot of δ_{aer} versus α shows the cluster shape observed for Tenerife,

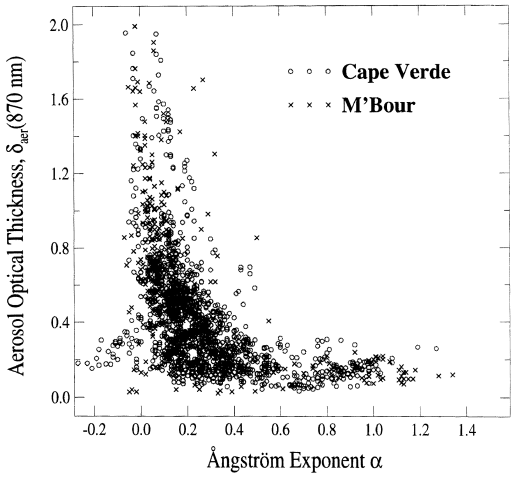

Fig. 6. Idem except that is representative of Cape Verde and M'Bour. While the scale of the *x*-axis is identical as the one of Fig. 5, the *y*-axis is 4 times increased.

although δ_{aer} goes up to 2.0 during dust events (up to a factor of 6 higher than in Tenerife). The Ångström exponent reaches 1.4 as maximal value, comparable to the maximum observed in Tenerife.

4. Methodology of the retrieval of the aerosol polarised phase function

Because sky-radiance measurements significantly depend on the experimental conditions such as solar zenith angle, topography of the site, quantity of aerosols, molecular contribution, etc., raw measurements are difficult to interpret for aerosol study. Therefore, as explained by Vermeulen (1996, 1999), given the aerosol optical thickness measured by the sunphotometers, we first remove multiple scattering effects from the measured polarised radiation. Then we subtract the molecular contribution to infer the aerosol polarised phase function which depends only on the aerosol characteristics (size distribution, refractive index, shape of the particle). This angular function represents the probability of the particles to scatter a polarised wave in the direction of the scattering angle. Because land-surface influence is negligible in the polarised downwards radiance (Bréon et al., 1995; Lafrance, 1997), we do not consider it in the data-processing. The method is extended to multispectral data. It is explained hereafter.

In the solar principal plane, for a homogeneous plane-parallel atmosphere, the relationship between the single-scattering polarised radiance $L^{(1)}_{pol}(\theta_d)$ and the aerosol polarised phase function $Q_a(\theta_d)$, at a fixed wavelength λ, is:

$$L^{(1)}_{pol}(\theta_d) = \frac{\pi L^{(1)*}_{pol}(\theta_d)}{E_S} = \frac{\bar{\omega}_0 \delta_{aer} Q_a(\theta_d) + \delta_{Ray} Q_R(\theta_d)}{\delta_{aer} + \delta_{Ray}} \times \frac{1}{4}\left[e^{-(\delta_{aer}+\delta_{Ray})/\mu_V} - e^{-(\delta_{aer}+\delta_{Ray})/\mu_S}\right] \times \frac{\mu_S}{\mu_S - \mu_V}. \quad (1)$$

The quantity $\bar{\omega}_0 Q_a(\theta_d)$, the product of the aerosol single scattering albedo, $\bar{\omega}_0$, and the polarised phase function, is the unknown variable. δ_{aer} is the aerosol optical thickness, measured by a sunphotometer. δ_{Ray} and $Q_R(\theta_d)$ are respectively the molecular optical thickness and the molecular polarised phase function, quantified by Rayleigh theory. $\mu_S = \cos\theta_S$, $\mu_V = \cos\theta_V$, where θ_S and θ_V are respectively the solar zenith angle and the viewing zenith angle.

In order to correct the measured polarised radiance of multiple scattering effects, numerical simulations of the ratio of single-to-multiple polarisation, $R^{S/M}(\theta_d, \bar{\omega}_0^{par}, \delta_{aer})$ are performed by using an arbitrary aerosol phase matrix $\boldsymbol{P}_a$ (defining the natural and the polarised phase functions $P_a^{par}(\theta_d)$ and $Q_a^{par}(\theta_d)$), an arbitrary aerosol single scattering albedo $\bar{\omega}_0^{par}$ and the measured aerosol optical thickness.

$$R^{S/M}(\theta_d, \bar{\omega}_0^{par}, \delta_{aer}) = \frac{L^{(1)}_{pol,calc}(\theta_d)}{L^{(n)}_{pol,calc}(\theta_d)}. \quad (2)$$

$L^{(1)}_{pol,calc}(\theta_d)$ is calculated by using the relation (1), $L^{(n)}_{pol,calc}(\theta_d)$ results of simulations by the radiative transfer code of Successive Orders OS (Deuzé et al., 1989).

Calculations of $R^{S/M}(\theta_d, \bar{\omega}_0^{par}, \delta_{aer})$ have been made at three wavelengths (445, 665, 870 nm), for a solar zenith angle of 60°. The arbitrary aerosol phase matrix is derived from an aerosol model following a Junge law, $n(r) = Cr^{-\nu}$ (r is the particle radius, C is a constant) with $\nu = 4.6$. However, the choice of the aerosol model is not important as the ratio $R^{S/M}(\theta_d, \bar{\omega}_0^{par}, \delta_{aer})$ proves to be nearly insensitive to the aerosol phase matrix (Vermeulen, 1996). Here, the aerosols are assumed to be non absorbing ($\bar{\omega}_0^{par} = 1$) and the aerosol optical thick-

ness is set to two values: δ_{aer} ($\lambda = 870$ nm) = 0.1 and δ_{aer} ($\lambda = 870$ nm) = 0.4. The curves are reported in Fig. 7. The angular variation of the ratio is very small in an angular interval of which the inferior boundary increases for shorter wavelengths. At large scattering angles the ratio increases because of the increase of the air mass for viewing zenith angles beyond 70°. At lower scattering angles the increase is due to a discontinuity of $R^{S/M}(\theta_d, \bar{\omega}_0^{par}, \delta_{aer})$. Indeed $L^{(n)}_{pol,calc}(\theta_d)$ (eq. (2)) is equal to 0 for a scattering angle included between 10° (at 870 nm) and 20° (at 445 nm). At a scattering angle of 80°, the ratio is included between 0.58 ($\lambda = 445$ nm and δ_{aer} ($\lambda = 870$ nm) = 0.4) and 0.9 ($\lambda = 870$ nm and δ_{aer} ($\lambda = 870$ nm) = 0.1). These relatively large values demonstrate that polarisation results mainly of single scattering. $R^{S/M}(\theta_d, \bar{\omega}_0^{par}, \delta_{aer})$ diminishes when δ_{aer} increases and when λ decreases.

Applying this ratio to the measurements provides the measured, polarised, single scattered radiance, $L^{(1)}_{pol,meas}$, from which molecular contribution $Q_R(\theta_d)$ ($Q_R(\theta_d) = \frac{3}{4}(1 - \cos^2(\theta_d))$ is subtracted in order to get $\bar{\omega}_0 \delta_{aer} Q_a^{retr}(\theta_d)$ (eq. (1)) which finally gives the retrieved polarised phase function multiplied by the aerosol single scattering albedo.

Devaux et al (1998) originally applied this method to the measured total radiance, for the retrieval of the aerosol single scattering albedo, $\bar{\omega}_0$, and of the natural phase function. However this procedure requires much more attention, especially concerning the influence of the surface reflectance and necessitates other photometric data. Because we do not get routinely the value of $\bar{\omega}_0$, for processing the whole set of data we need to fix arbitrarily a value for $\bar{\omega}_0^{par}$. It is set equal to 1 (its maximal value). Thus $Q_a^{retr}(\theta_d)$ is reduced to its minimal value. Indeed, decreasing $\bar{\omega}_0^{par}$ makes $L^{(n)}_{pol,calc}(\theta_d)$ decrease quicker than $L^{(1)}_{pol,calc}(\theta_d)$. And consequently both $R^{S/M}(\theta_d, \bar{\omega}_0^{par}, \delta_{aer})$ and $Q_a^{retr}(\theta_d)$ increase. Calculations with $\bar{\omega}_0^{par} = 0.8$ on the available data show $Q_a^{retr}(\theta_d)$ may increase by 30–40% at 870 nm, by up to 200% at 445 nm during the dust events (when the polarised phase function is small).

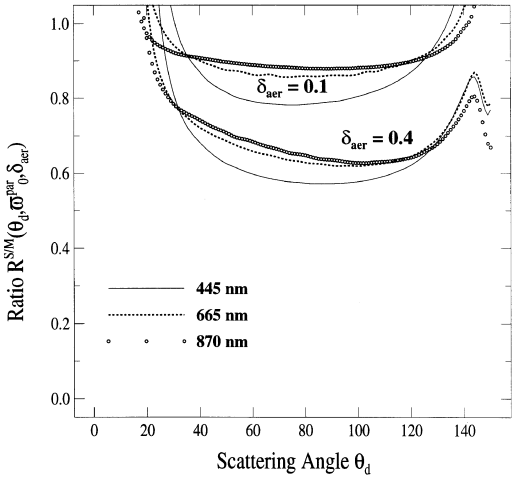

Fig. 7. Ratio of single-to-multiple polarisation $R^{S/M}(\theta_d, \bar{\omega}_0^{par}, \delta_{aer})$ as a function of the scattering angle θ_d, for 2 values of the aerosol optical thickness δ_{aer} (0.1 and 0.4) and at 3 wavelengths.

Numerical solutions, from OS, are conducted for the vertical density profiles of aerosols and molecules, described by two height scales. The aerosol effect is parameterised through a phase matrix, the aerosol single scattering albedo and the aerosol optical thickness, the molecules by the Rayleigh phase matrix and the molecular optical thickness. The surface albedo has negligible influence on downward polarisation calculations. More details about this code can be found in Deuzé et al. (1989), and for its application to this study, in Vermeulen (1996) and in Devaux et al. (1998). Because the code assumes a plane parallel atmosphere, the angular limitation of the algorithm for the viewing angle is 80° where the effect of non sphericity is relevant (Vermote and Tanré, 1992).

The uncertainty of results depends on δ_{aer}, on the aerosol model defined as algorithm-parameter, on the measurement wavelength and on the scattering angle. In the conditions of a dust event ($\delta_{aer}(870\text{ nm}) = \delta_{aer}(445\text{ nm}) = 0.2$) the uncertainty on the retrieved polarised phase function at 60° is around 0.01 at 870 nm and 0.05 at 445 nm. During clear days ($\delta_{aer}(870\text{nm}) = 0.02$; $\delta_{aer}(445\text{nm}) = 0.05$), it increases up to 0.07 at 870 nm, up to 0.2 at 445 nm.

5. Application to RefPol and CIMEL measurements

5.1. *Tenerife*

Polarised phase functions derived from combined RefPol and sunphotometer measurements acquired at 870 nm are plotted in Fig. 8 for 4

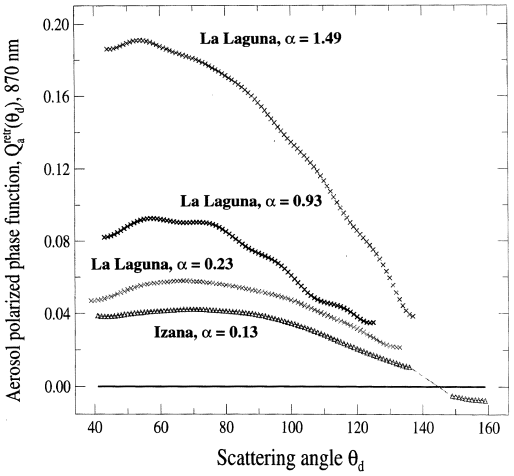

Fig. 8. Inferred polarised phase functions at 870 nm for 4 different Ångström exponents α. The two smaller values of α correspond to dust events in La Laguna and Izaña (8 July morning and 17 July afternoon respectively). The two others correspond to measurements acquired in La Laguna during clear days (30 June afternoon and 1 July).

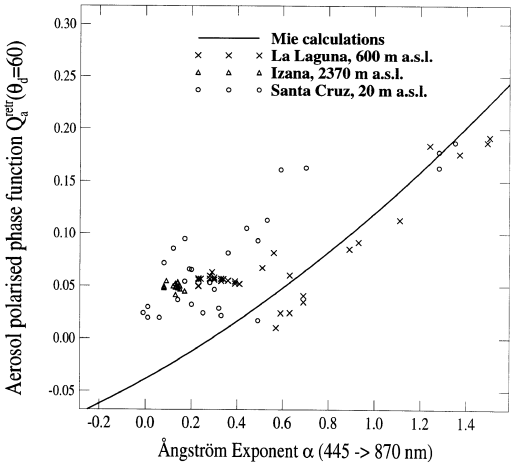

Fig. 9. The polarised phase function retrieved at 870 nm and at a scattering angle of 60°, is shown versus the Ångström exponent, derived from spectral extinction measurements simultaneous to the measured polarised sky-radiances. Numerical calculations by Mie theory are added for comparison.

values of the Ångström exponent α. The measurements can not be used for scattering angles lower than 20° because of solar perturbations, neither for viewing zenith angles larger than 70° in La Laguna, 80° at Izaña, because of the encumbrance of the horizons.

The maximum of the phase functions is reached at around 60° and its magnitude varies between 0.04 and 0.20. During the dust episodes, the phase function reaches negative values at large scattering angles (greater than 140°). As observed in Fig. 8, the polarised phase function depends strongly on the Ångström exponent, as also pointed out theoretically by Bréon et al. (1997). To verify this behaviour on the whole set of data, we plot in Fig. 9 the polarised phase function at 60° versus the Ångström exponent. This angle is chosen because it corresponds to a maximum of the signal and because the influence of the particle refractive index, not measurable directly by our measurements, is small. Data corresponding to clear conditions at Izaña are not included in Fig. 9, as the aerosol optical thickness is close to the instrumental detection limit. The strong correlation between the spectral atmospheric extinction and the aerosol polarisation properties is evident, although the two measurements are independent from each other. For small α, corresponding to large particles (during the dust episodes), the polarisation level is close to zero. It increases for increasing α, up to $Q_a^{retr}(60°) = 0.2$ for $\alpha = 1.5$, in La Laguna and during clear conditions. Therefore, small particles polarise more than big particles.

The strong influence of polarisation by small particles is noticeable even when restricting the analysis to clear conditions only (α greater than 0.5 in Fig. 9). This is shown for La Laguna, where an increase of α is correlated to an increase of $Q_a^{retr}(60°)$ in correspondence of low δ_{aer} values. Indeed at La Laguna, a sudden increase in the polarised phase function $Q_a^{retr}(60°)$ (a factor of 2 in 90 min) is observed on 30 June afternoon when α varied simultaneously between 0.93 and 1.50. $Q_a^{retr}(60°)$ then remains stable until the morning after (as α). On the same period, despite a gap of 28 h during which no measurements are available, an increase of the same order is noticed at Santa Cruz. By making no distinction between the locations, the atmosphere seems stable until 30 June, at 17:00 GMT, then a rapid change occurs in 90 min, after which the situation stays stable along the day after, until the afternoon. The first measurements possible in La Laguna and Santa Cruz after this episode were made on 5 July and 6 July respectively, which showed a polarisation level

still lower than on 30 June morning. All these changes of $Q_a^{retr}(60^\circ)$ are correlated with changes of α.

On Fig. 9 are reported numerical calculations (by Mie theory) of $Q_a^{retr}(60^\circ)$ versus α, by assuming a Junge law for the size distribution. The slope v is varied between 2.8 and 4.5 to obtain values of α ranging between -0.2 and 1.5 ($v = \alpha + 3$). Calculations have been conducted for several values of the refractive index m. The small influence of m on calculated quantities makes possible to draw a single curve (as plotted in Figs. 9, 10). Measurements and calculations are correlated for large values of α. Measurements show that, during dust events, large particles polarise more than the theoretical predictions.

5.2. *Cape Verde and M'Bour*

The same analysis has been applied to the measurements acquired by AERONET in Cape Verde and M'Bour. As measurements are performed automatically, particular care is taken in discriminating unperturbed cloudless conditions. Data are thus filtered first with respect to retrieved aerosol optical thickness values and then with respect to total radiance measured in the solar principal plane. The first test filters out measurements for which the variance of aerosol optical thickness acquired during one hour is greater than 12%. The test on total radiance eliminates the angular parts where the curve presents peaks due to scattering by clouds. The filter on δ_{aer} eliminates 70% of the available measurements in Cape Verde, 60% in M'Bour. The filter on the total radiance eliminates about 6% of the δ_{aer}-filtered data. 4% of the data are further eliminated when considered not physical (excessively high or negative values). Eventually, about 20% of the Cape Verde measurements and 30% of M'Bour measurements are processed, yielding more than 500 principal plane data sets.

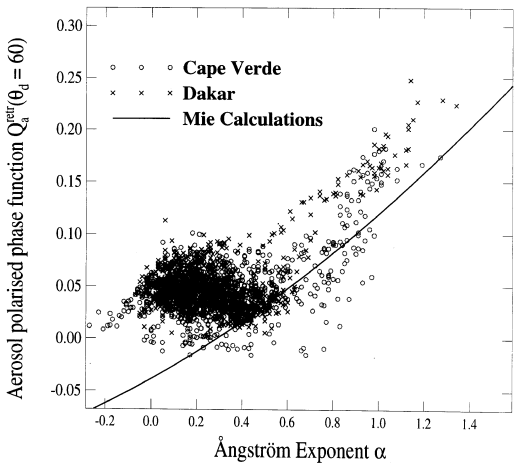

Fig. 10. Same as Fig. 9 except for M'Bour and Cape Verde. The axis scales in both figures are identical. The same Mie calculations as in Fig. 9 are included.

A good correlation between $Q_a^{retr}(60)$ and α is obtained (Fig. 10). As observed in Tenerife, $Q_a^{retr}(60^\circ)$ for dust episodes ranges from 0 to 0.1, while for smaller particles ($0.8 < \alpha < 1.4$) $Q_a^{retr}(60^\circ)$ varies between 0.1 and 0.25. However the scatter of the points indicates that polarisation does not depend uniquely on the aerosol Ångström exponent.

6. Spectral characteristics of the polarised phase function

The same procedure is used for the polarised sky-radiance measured at 445 nm at Tenerife by RefPol. Polarisation measurements at 445 nm are necessary to validate the POLDER observations, and were operated at this wavelength for the first time at this occasion in Tenerife and in Lille (north of France). Measurements in Lille are not discussed in this paper, but the authors are currently working on these data.

The polarised phase functions retrieved from simultaneous measurements at 445 and 870 nm are plotted in Figs. 11, 12. Fig. 11 corresponds to acquisitions in La Laguna and Izaña during dust events. Fig. 12 corresponds to measurements made in La Laguna during clear conditions.

As observed at 870 nm, the polarised phase function at 445 nm is much smaller during dust events ($Q_a^{retr}(\theta_d)$ always lower than 0.05) than under clear conditions ($Q_a^{retr}(\theta_d)$ up to 0.40). During dust event, $Q_a^{retr}(\theta_d)$ even presents a sign inversion. This feature is much clearer than at 870 nm, and it occurs at 95° in La Laguna and at 105° in Izaña. The maximum of the phase function at 870 nm occurs between 50° and 80°, while it tends towards smaller angles at 445 nm, specially during dust events.

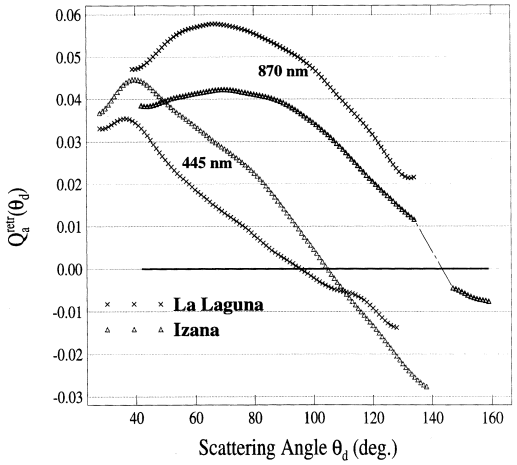

Fig. 11. Polarised phase functions versus the scattering angle at 445 nm and at 870 nm, inferred from 2 measurements acquired in Izaña and La Laguna during dust events (17 June afternoon and 8 July morning, respectively).

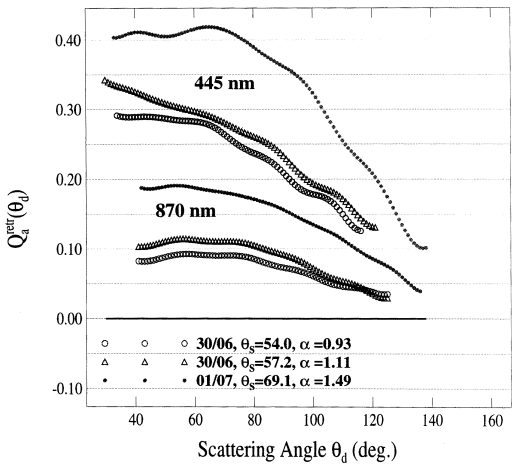

Fig. 12. Same as Fig. 11 except that the curves are the results of 3 measurements acquired during clear days in La Laguna only (30 June, 1 July).

The spectral dependence changes from clear to dusty conditions. In the first case, the polarised phase function is higher at 445 nm than at 870 nm, while during dust event, $Q_a^{retr}(\theta_d)$ is higher at 870 nm. In Fig. 13, the dependence of $Q_a^{retr}(60^\circ)$ at 445 nm and 870 nm is plotted against the Ångström exponent α. Error bars are added for sparse values of α, randomly selected. While the same correlation with respect to α appears within the error bars, the spectral dependence is questionable because of the uncertainties both for clear and dusty conditions.

On 30 June and 1 July, the polarised phase function at 445 nm in La Laguna increases by a factor of around 2, as does the polarised phase function at 870 nm (discussed previously), and even in this case, the correlation with α remains good.

7. Comparisons with size distribution retrievals

In order to test the implications of our polarisation data, we used an AERONET-inverted size distribution (Smirnov et al, 1998) to perform radiative transfer simulations and compare the calculations with the polarisation measurements. On 17 July afternoon, during the 2nd dust event, RefPol and a CIMEL instrument simultaneously acquired photometric data at Izaña, along with instruments onboard the Pelican aircraft (Schmid et al., 2000) which performed a vertical profile directly above Izaña in the late afternoon.

The refractive index associated with the inverted size distribution is $m = 1.45–0.005$.i. Mie calculations of the resulting phase matrix show that the predicted polarised phase function is very close to zero, and even negative, as is shown in Figs. 14, 15. Calculations for other values of real and imaginary parts of the refractive index do not show significant changes of the aerosol polarising properties. The polarised phase function derived from RefPol measurements are compared with these calculations in Figs.14, 15. At 445 and 870 nm, our results show that the aerosols exhibit positive polarisation (i.e., Rayleigh type). Nevertheless the polarised phase function is very low and the maximum reaches 0.04. Multispectral measurements show different polarising properties to what is predicted by Mie theory and total radiance processing (Smirnov et al., 1998).

From airborne in-situ measurements onboard the Pelican, Öström and Noone (2000) provided values of the dry aerosol single scattering albedo at several altitudes. Above Izaña, at 3250 m a.s.l., they obtained 0.89 ± 0.1, and 0.83 ± 0.36 at 3885 m a.s.l. From other photometric measurements

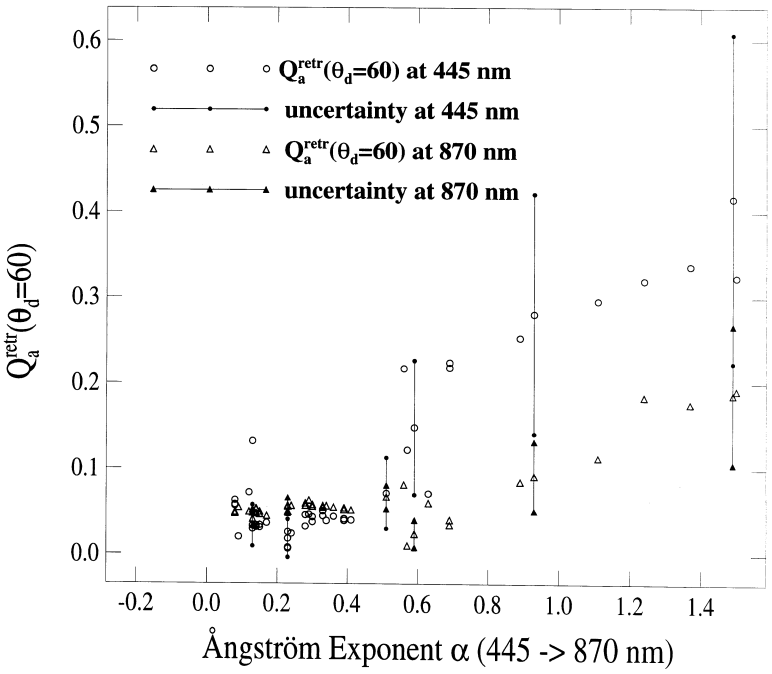

Fig. 13. Polarised phase functions at 60°, at 445 and 870 nm, versus α, retrieved from measurements in Tenerife. The error bars (for clarity, only few have been added) show that the large uncertainty of results at 445 nm prevents to draw definite conclusions on the spectral dependence of the polarised phase function but confirms the dependence on α, at 445 nm and at 870 nm.

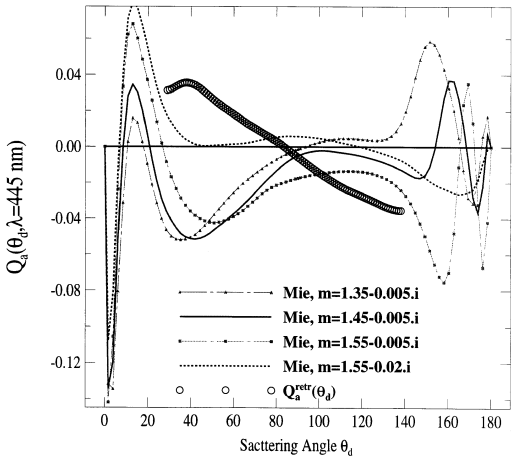

Fig. 14. Polarised phase function at 445 nm versus the scattering angle as calculated by Mie theory for the AERONET size distribution, for several values of the refractive index, and as retrieved from the measured polarised sky-radiance. The measurements were acquired at Izaña on 17 June afternoon during a dust event.

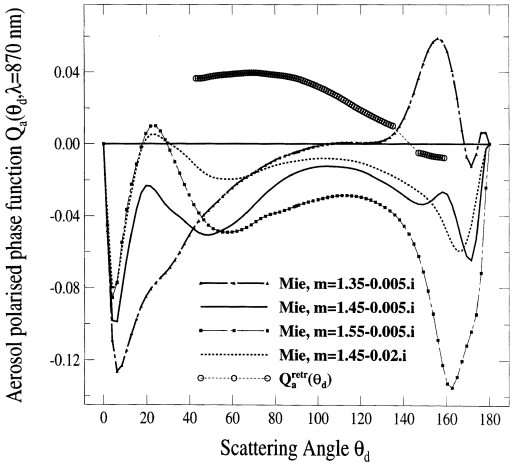

Fig. 15. Idem as Fig. 13 except that the wavelength is 870 nm.

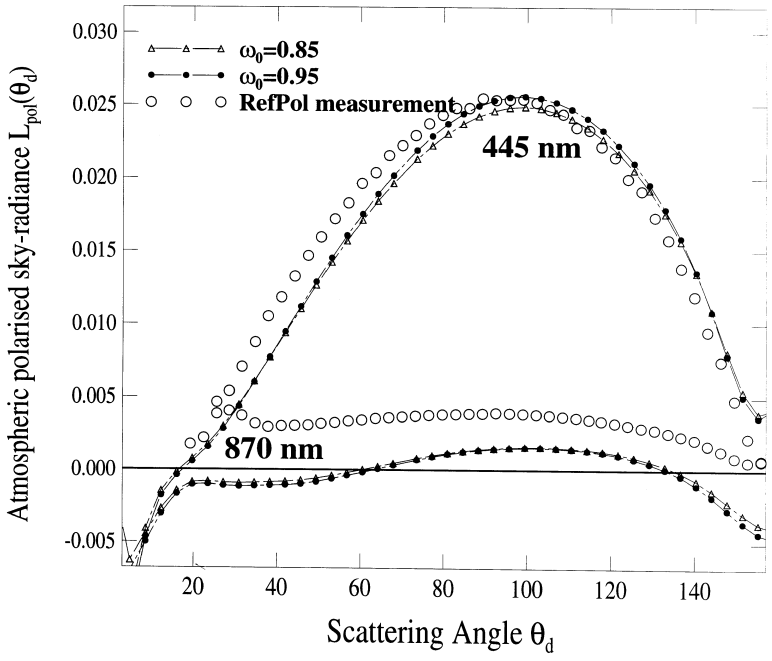

Fig. 16. Polarised sky-radiance versus the scattering angle θ_d as measured by RefPol at 445 and 870 nm at Izaña on 17 July, 18:26, and as calculated by the radiative transfer code OS for the experimental conditions (δ_{aer}, θ_S, ...) and for the size distribution inverted from AERONET measurements. $\bar{\omega}_0^{par}$ is set equal to 2 values: 0.85 and 0.95.

performed at "Pico Del Teide" (28°16′N, 16°36′W, 3570 m a.s.l.), situated higher than Izaña, not far from the summit of the mountain, Formenti et al (2000) derived for the same day an ambient $\bar{\omega}_0$ value of 0.89 ± 0.32 (morning average). As the aerosol optical thickness is measured by the AERONET instrument, all parameters are available for simulating the downward polarised sky-radiance from the radiative transfer code OS. For representing the range of measured $\bar{\omega}_0$, we use two values: 0.85 and 0.95. The atmospheric polarised sky-radiance, as measured by RefPol at 445 and 870 nm and as simulated for the two values of $\bar{\omega}_0$, are plotted in Fig. 16. While the order of magnitude of the simulation and the measurement are similar at 445 nm (due to large molecular contribution), the discrepancy is very large at 870 nm. Measurements show atmospheric polarisation is larger than predicted by the simulations at this latter wavelength. Decreasing the aerosol single scattering albedo is not sufficient to fill the gap. Another cause of the disagreement might be due to the quantity of particles. However the aerosol optical thickness, directly proportional to the number of aerosols, is measured with a good precision. As we demonstrated earlier, the effect of small particles on polarisation is bigger than the effect of big particles, therefore the change in the size distribution by increasing the number of small particles with respect to the bigger particles would increase the polarisation. A likely cause of disagreement is the presence, at the height of Izaña, of a thin layer of small particles which is advected from the MBL along the mountain ridge of Izaña by upslope thermal winds (Raes et al., 1997; Welton et al., 2000). The quantification of the effect of upslope particles on the total and the polarised radiances can be achieved by adding the size distributions measured in-situ at Izaña to the inverted size distributions. Work on this issue is currently in progress.

8. Conclusion

Multispectral measurements of atmospheric polarisation were acquired in Tenerife, at three altitudes, during clear days and during the 2 first dust events which occurred during ACE-2.

Measured aerosol optical thickness is used in numerical calculations for correcting the polarised sky-radiance of the effect of multiple scattering. Then the molecular contribution is subtracted in order to provide the polarised phase function, which depends only on the aerosol characteristics. Results inferred at 870 nm from data acquired in Tenerife and in two AERONET sites located in the same geographical area, show that the aerosol polarised phase function is very well correlated with the Ångström exponent α, derived from independent measurements of spectral solar extinction. The uncertainty on retrievals at 445 nm, larger than at 870 nm because of the large contribution of molecular scattering to the total signal at 445 nm, prevents a definite conclusion on the spectral dependence of the polarised phase function. Nevertheless, even at 445 nm, the good correlation with α is observed. The correlation shows that small particles polarise more than large particles. The accuracy of the calibration coefficients should be improved to be reduced down to 1% in order to draw definite conclusions on the spectral dependence of the polarised phase function.

The preliminary step of a case study shows that polarisation contains information on size distribution that total radiance does not provide. More precisely, the present analysis indicates that applying Mie theory calculations (spherical particles), to desert aerosols, tends to underestimate the effect of small, very polarising aerosols.

For our study, it was convenient to concentrate on the polarised phase function for a scattering angle of 60° only because it depends little on the refractive index. However, as shown by Vermeulen (1996), analysing data at other angles allows better estimate of the aerosol size distribution and gives an evaluation of the real part of the refractive index. Work is currently ongoing about inversion of whole set of data (including total sky-radiance measured in the almucantar and solar principal plane geometry, spectral extinction measurements and polarisation measured in the solar principal plane at three wavelengths). In this way the size distribution, for aerosol diameters extending from 0.1 to 20 μm, can be inferred as well as the spectral variation of the real part of aerosol refractive index, integrated in the whole atmospheric column.

9. Acknowledgements

AERONET and Photons teams are acknowledged for providing AERONET data, and particularly B. Chatenet, J.-B. Defossez, B. Holben, F. Lavenu, A. Smirnov, D. Tanré, J. Welton. TE is grateful to P. Formenti for precious comments and critics, and to Karin Seron for encouragement.

REFERENCES

Arimoto, R., Duce, R. A., Ray, B. J., Ellis Jr., W. G., Cullen, J. D. and Merrill, J. T. 1995. Elements in the atmosphere over the North Atlantic. *J. Geophys. Res.* **100**, 1199–1213.

Bréon, F.-M., Tanré, D., Lecomte, P. and Herman, M. 1995. Polarized reflectance of bare soils and vegetations: measurements and models. *IEEE Trans. Geosci. Remote Sensing* **33**, 487–499.

Bréon, F.-M., Deuzé, J.-L., Tanré, D. and Herman, M. 1997. Validation of spaceborne estimates of aerosol loading from sunphotometer measurements with emphasis on polarization. *J. Geophys. Res.* **102**, 17187–17195.

Cairns, B., Travis, L. D. and Russell, E. E. 1997. An analysis of ground-based polarimetric sky radiance measurements. *Proc. SPIE* **3220**, 103–114.

Charlson, R. J., Schwartz, S. E., Hales, J. M., Cess, R. D., Coakley Jr, J. A., Hansen, J. E. and Hofmann, D. J. 1992. Climate forcing by anthropogenic aerosols. *Science* **255**, 423–430.

Chiapello, I., Bergametti, G., Chatenet, B., Bousquet, P., Dulac, F. and Santos Soares, E. 1997. Origins of African dust transported over the northeastern tropical Atlantic. *J. Geophys. Res.* **102**, 13701–13709.

Chiapello, I., Bergametti, G., Chatenet, B., Dulac, F., Moulin, C., Vermeulen, A., Devaux, C., Jankowiak, I. and Santos Soares, E. 1999. Contribution of the different aerosol species to the aerosol mass load and optical depth over the northeastern tropical Atlantic. *J. Geophys. Res.* **104**, 4025–4035.

Deschamps, P. Y., Bréon, F. M., Leroy, M., Podaire, A., Bricaud, A., Buriez, J. C. and Sèze, G. 1994. The POLDER mission: instrument characteristics and scientific objectives. *I.E.E.E. Trans. Geosci. Remote Sens.* **32**, 598–615.

Deuzé, J.-L., Herman, M., Santer, R. 1989. Fourier series expansion of the transfer Equation in the atmosphere–ocean system. *J. Quant. Spectrosc. Radiat. Transfer* **41**, 483–494.

Deuzé, J. L., Bréon, F. M., Deschamps, P. Y., Devaux, C.

and Herman, M. 1993. Analysis of the POLDER (POLarization and Directionality of Earth Reflectance) airborne instrument observations over land surfaces. *Remote Sens. Environ.* **45**, 137–154.

Devaux, C., Vermeulen, A., Deuzé, J.-L., Dubuisson, P., Herman, M. and Santer, R. 1998. Retrieval of aerosol single scattering albedo from ground-based measurements: Application to observational data. *J. Geophys. Res.* **103**, 8753–8761.

Formenti, P., Andreae, M. O. and Lelieveld, J. 2000. Measurements of Aerosol Optical Depths in the North Atlantic Free Troposphere: results from ACE-2. *Tellus* **52B**, 678–693.

Hansen, J. E. and J. W. Hovenier. 1974. Interpretation of the polarization of Venus. *J. Atmos. Sci.* **31**, 1137–1160.

Herman, M., Deuzé, J. L., Devaux C., Goloub, P., Bréon F. M. and Tanré, D. 1997. Remote sensing of aerosols over land surfaces including polarisation measurements and application to POLDER measurements. *J. Geophys. Res.* **102**, 17039–17049.

Holben, B. N., Eck, T. F., Slutsker, I., Tanré, D., Buis, J. P., Setzer, A., Vermote, E., Reagan, J. A., Kaufman, Y. J., Nakajima, T., Lavenu, F., Jankowiak, I. and Smirnov, A. 1998. AERONET — A federated instrument network and data archive for aerosol characterisation. *Remote Sens. Environ.* **66**, 1–16.

Lafrance, B. Sept. 1997. Modélisation simplifiée de la lumière polarisée émergeant de l'atmosphepe. Correction de l'impact des aérosols stratosphériques sur les mesures de POLDER. Thèse de l'Univ. des Sci. et Technol. de Lille, Lille, France.

Lenoble, J. 1993. *Atmospheric radiative transfer* A. Deepack Publishing, 532 pp.

Mishchenko, M. I. and Travis, L. D. 1997. Satellite retrieval of aerosol properties over the ocean using polarization as well as intensity of reflected sunlight. *J. Geophys. Res.* **102**, 16989–17013.

Nakajima, T., Tonna, G., Rao, R., Boi, P., Kaufman, Y. J. and Holben, B. N. 1996. Use of sky-brightness measurements from ground for remote sensing of particulate dispersions. *Appl. Opt.* **35**, 2672–2686.

Öström, E. and Noone, K. 2000. Vertical profiles of aerosol scattering and absorption measured in situ during the north atlantic Aerosol Characterization Experiment. *Tellus* **52B**, 526–545.

Prospero, J. M. and Carlson, T. N. 1972. Vertical and areal distribution of Saharan dust over the western equatorial North Atlantic ocean. *J. Geophys. Res.*, **77**, 5255–5265.

Raes F., Van Dingenen, R., Cuevas, E., Van Velthoven, P. F. J. and Prospero, J. M. 1997. Observations of aerosols in the free troposphere and marine boundary layer of the subtropical Northeast Atlantic: discussion of processes determining their size distribution. *J. Geophys. Res.* **102**, 21,315–21,328.

Raes, F., Bates, T., Mac Govern, F. M. and Van Liedekerke, M. 2000. The second Aerosol Characterization Experiment (ACE-2): General overview and main results. *Tellus* **52B**, 111–126.

Russell, P. B. and Heintzenberg, J. 2000. An overview of the ACE 2 Clear Sky Column Closure Experiment (CLEARCOLUMN). *Tellus* **52B**, 463–483.

Smirnov, A., Holben, B. N., Slutsker, I., Welton, E. J. and Formenti, P. 1998. Optical properties of Saharan dust during ACE-2. *J. Geophys. Res.* **103** 28,079–28,092.

Schmid, B., Livingston, J. M., Russell, P. B. Durkee, P. A., Jonsson, H., Collins, D. R., Flagan, R. C., Seinfeld, J. H., Gass, S., Hegg, D. A., Öström, E., Noone, K. J., Welton, E. J., Voss, K. J., Gordon, H. R., Formenti, P. and M. O. Andreae. 2000. Clear sky closure studies of lower tropospheric aerosol and water vapor during ACE-2 using airborne sunphotometer, airborne in-situ, space-borne, and ground-based measurements. *Tellus* **52B**, 568–593.

Tegen, I. and Lacis, A. A. 1996. Modeling of particle size distribution and its influence on the radiative properties of mineral dust aerosol. *J. Geophys. Res.* **101**, 19237–19244.

Van de Hulst, H. C. 1957. *Light scattering by small particles*. John Wiley, New York, USA, 470 pp.

Vermeulen, A. 1996. Caractérisation des aérosols à partir de mesures optiques passives au sol: Apport des luminances totale et polarisée dans le plan principal, Thése de l'Univ. des Sci. et Technol. de Lille, Lille, France.

Vermeulen, A., Devaux, C. and Herman, M. 1999. Retrieval of the phase function and the polarized phase function of aerosols from ground-based measurements. *Proceedings of the International Conference and Workshops on Ocean Color, Land Surfaces, Radiation and Clouds, Aerosols, ALPS'99*. The contribution of POLDER and new generation spaceborne sensors to global change studies, WK1-O-20.

Vermote, E. and Tanré, D. 1992. Analytical expressions for radiative properties of planar Rayleigh scattering media, including polarization contributions. *J. Quant. Spectros. Radiat. Transfer* **47**, 305–314.

Verver, G., Raes, F., Vogelezang, D. and Johnson, D. 2000. The second Aerosol Characterization Experiment (ACE-2): Meteorological and chemical context. *Tellus* **52B**, 126–140.

Welton, E. J., Voss, K. J., Gordon, H. J., Maring, H, Smirnov, A., Holben, B. N., Schmid, B, Livingston, J. M., Russell, P. B., Durkee, P. A., Formenti, P. and Andreae, M. O. 2000. Ground-based Lidar Measurements of Aerosols During ACE-2: Instrument Description, Results, and Comparisons with other Ground-based and Airborne Measurements. *Tellus* **52B**, 636–651.